We are IntechOpen, the world's leading publisher of Open Access books Built by scientists, for scientists

6,900
Open access books available

185,000
International authors and editors

200M
Downloads

Our authors are among the

154
Countries delivered to

TOP 1%
most cited scientists

12.2%
Contributors from top 500 universities



WEB OF SCIENCE™

Selection of our books indexed in the Book Citation Index in Web of Science™ Core Collection (BKCI)

Interested in publishing with us?
Contact book.department@intechopen.com

Numbers displayed above are based on latest data collected.
For more information visit www.intechopen.com



Chapter

Induction Electrical Machine Simulation at Three-Phase Stator Reference Frame: Approach and Results

Mikhail Pustovetov

Abstract

This chapter provides the equations of mathematical model of three-phase induction electrical machine recorded in the three-phase stator reference frame. The possibilities of the proposed mathematical model are described in detail. This chapter also discusses the development of the computer model of an induction motor based on the abovementioned mathematical model. It uses an approach that allows combining during preparation the computer model dual methods: means of visual programming circuitry (in the form of electrical schematics) and logical one (in the form of block diagrams). The approach enables easy integration of the model of an induction motor as part of more complex models of electrical complexes and systems. The developed computer model gives the user access to the beginning and the end of a winding of each of the three phases of the stator and rotor. This property is particularly important when considering the asymmetric modes of operation or when powered by the special circuitry of semiconductor converters. Simulation results show the adequacy of the proposed mathematical model of induction electrical machine.

Keywords: induction electrical machine, mathematical model, stator reference frame, electromagnetic torque, instantaneous power, simulation

1. Introduction

The induction motor (IM) plays a very important role in industrial sectors and transport, primarily due to its robustness and low cost. There are some authors, who devote their publications to problems of mathematical modeling of IM [1–6]. The author wishes to offer its own version of a mathematical model (MM) of the IM, suitable for unbalanced modes of simulation purposes.

Writing the equations of the MM of a three-phase IM in a three-phase stator reference frame (SRF) is useful in the analysis, comparing the calculated and actual curves of currents and phase voltages, suitable without additional transformation of equations for the consideration of modes of IM operation at asymmetrical characteristics of feed or parameters of IM. Simulation results for the coordinatesα, β, γ correspond to the actual processes in phases A, B, and C of the stator, in the case of the short-circuited rotor, i.e., in most cases, only and can be experimentally

measured. IM simulation in three-phase coordinates is useful in detecting and diagnosing defects in the stator [3] and implementing algorithms for direct torque control.

It can be argued—subject to review only, the fundamental spatial harmonics of the magnetic field in the air gap is symmetrical in a construction three-phase IM, powered by non-sinusoidal voltages asymmetrical system—that simulation results will be correct, but the same one in two-phase orthogonal coordinates will not.

2. Mathematical model equations

The suggested MM of a three-phase IM is based on a three-phase electrical machine MM at SRF coordinate system axis α, β, γ [5], which are aligned with the stator phase axes A, B, and C. This basic MM supplemented by iron losses resistances r_μ included in magnetization circuits in each phase of IM in parallel with magnetizing inductance L_μ [6] (analogy with the T-shaped equivalent circuit of induction electric machine). The equations of the electromagnetic processes in IM are given in Eq. (1), adopted by the usual generalized electrical machine assumptions: each of the phase stator windings creates in a smooth air gap in the sinusoidal-allocated magnetomotive force; magnetic saturation coefficient is constant. In the expressions (Eq. (1)), the following notations are further adopted: v, voltage; i, current; t, time; r, resistance; Ψ, magnetic flux linkage; ω_r, mechanical rotor speed; and p, the number of pole pairs. Lower indexes α, β, γ indicate the affiliation to the appropriate phase. The subscript s indicates the affiliation to the stator, the index r belongs to the rotor, and index μ belongs to the magnetization branch. $L_{\sigma s\alpha}$ is the leakage inductance of stator phase; $L_{\sigma r\alpha}$ is the leakage inductance of the rotor winding phase.

Traditionally, the rotor parameters are given to the stator winding. Detailed components of the system (Eq. (1)) are described in Eqs. (2)–(7). The form of Eq. (1) as much as possible is unified with published equations (Eq. (1)) of a three-phase transformer MM [7]:

$$\begin{cases} v_{s\alpha} = r_{s\alpha} i_{s\alpha} + \dfrac{d(L_{\sigma s\alpha} i_{s\alpha})}{dt} + v_{0\alpha}; & i_{\mu\alpha_active} = \dfrac{v_{0\alpha}}{r_{\mu\alpha}}; \\ v_{s\beta} = r_{s\beta} i_{s\beta} + \dfrac{d(L_{\sigma s\beta} i_{s\beta})}{dt} + v_{0\beta}; & i_{\mu\beta_active} = \dfrac{v_{0\beta}}{r_{\mu\beta}}; \\ v_{s\gamma} = r_{s\gamma} i_{s\gamma} + \dfrac{d(L_{\sigma s\gamma} i_{s\gamma})}{dt} + v_{0\gamma}; & i_{\mu\gamma_active} = \dfrac{v_{0\gamma}}{r_{\mu\gamma}}; \\ v_{r\alpha} = e_{0\alpha} - e_{rot\alpha} - \dfrac{d(L_{\sigma r\alpha} i_{r\alpha})}{dt} - r_{r\alpha} i_{r\alpha}; \\ v_{r\beta} = e_{0\beta} - e_{rot\beta} - \dfrac{d(L_{\sigma r\beta} i_{r\beta})}{dt} - r_{r\beta} i_{r\beta}; \\ v_{r\gamma} = e_{0\gamma} - e_{rot\gamma} - \dfrac{d(L_{\sigma r\gamma} i_{r\gamma})}{dt} - r_{r\gamma} i_{r\gamma}; \end{cases} \quad (1)$$

Voltages at the terminals of phase magnetization branches (derived from flux linkage of mutual induction)

$$v_{0\alpha} = \frac{d\Psi_{\mu\alpha}}{dt} = r_{\mu\alpha}\left[(i_{s\alpha} + i_{r\alpha}) - \frac{1}{2}\left(i_{s\beta} + i_{r\beta} + i_{s\gamma} + i_{r\gamma}\right) - \frac{\Psi_{\mu\alpha}}{M}\right];$$

$$v_{0\beta} = \frac{d\Psi_{\mu\beta}}{dt} = r_{\mu\beta}\left[\left(i_{s\beta} + i_{r\beta}\right) - \frac{1}{2}\left(i_{s\alpha} + i_{r\alpha} + i_{s\gamma} + i_{r\gamma}\right) - \frac{\Psi_{\mu\beta}}{M}\right]; \quad (2)$$

$$v_{0\gamma} = \frac{d\Psi_{\mu\gamma}}{dt} = r_{\mu\gamma}\left[\left(i_{s\gamma} + i_{r\gamma}\right) - \frac{1}{2}\left(i_{s\alpha} + i_{r\alpha} + i_{s\beta} + i_{r\beta}\right) - \frac{\Psi_{\mu\gamma}}{M}\right].$$

Mutual inductance of IM windings defined as

$$M = (2/3)L_{\mu} \quad (3)$$

M—mutual inductance of the phase windings of the rotor and stator of IM in the case of coincidence of their axes. In other words main inductance of the winding of the stator when magnetic flux calculated in the absence of currents in other phases of the stator and rotor windings (i.e., from the part of main magnetic flux created by the stator phase itself).

L_{μ}—complete phase inductance of the stator winding from the main magnetic flux, which takes into account the presence of currents in other phases. In other words the inductance of the main magnetic flux part is created by the winding itself M, and the inductance of the portion of the main magnetic flux is created by two other stator windings $M/2$.

Per-phase magnetizing currents:

$$\begin{aligned} i_{\mu\alpha} &= i_{s\alpha} + i_{r\alpha} = \frac{2}{3}\left[\left(i_{s\alpha} - \frac{1}{2}\left(i_{s\beta} + i_{s\gamma}\right)\right) + \left(i_{r\alpha} - \frac{1}{2}\left(i_{r\beta} + i_{r\gamma}\right)\right)\right] \\ &= i_{\mu\alpha_active} + i_{\mu\alpha_reactive}; \\ i_{\mu\beta} &= i_{s\beta} + i_{r\beta} = \frac{2}{3}\left[\left(i_{s\beta} - \frac{1}{2}\left(i_{s\alpha} + i_{s\gamma}\right)\right) + \left(i_{r\beta} - \frac{1}{2}\left(i_{r\alpha} + i_{r\gamma}\right)\right)\right] \\ &= i_{\mu\beta_active} + i_{\mu\beta_reactive}; \\ i_{\mu\gamma} &= i_{s\gamma} + i_{r\gamma} = \frac{2}{3}\left[\left(i_{s\gamma} - \frac{1}{2}\left(i_{s\alpha} + i_{s\beta}\right)\right) + \left(i_{r\gamma} - \frac{1}{2}\left(i_{r\alpha} + i_{r\beta}\right)\right)\right] \\ &= i_{\mu\gamma_active} + i_{\mu\gamma_reactive}. \end{aligned} \quad (4)$$

In the expressions (Eq. (4)), i_{μ_active} and $i_{\mu_reactive}$ are active and reactive (inductive) components of per-phase magnetizing current, respectively.

$$\begin{aligned} e_{0\alpha} &= -v_{0\alpha}; \\ e_{0\beta} &= -v_{0\beta}; \\ e_{0\gamma} &= -v_{0\gamma}. \end{aligned} \quad (5)$$

$$\begin{aligned} e_{rot\alpha} &= \frac{\left(\Psi_{r\beta} - \Psi_{r\gamma}\right)p\omega_r}{\sqrt{3}}; \\ e_{rot\beta} &= \frac{\left(\Psi_{r\gamma} - \Psi_{r\alpha}\right)p\omega_r}{\sqrt{3}}; \\ e_{rot\gamma} &= \frac{\left(\Psi_{r\alpha} - \Psi_{r\beta}\right)p\omega_r}{\sqrt{3}}. \end{aligned} \quad (6)$$

Flux linkages of IM rotor phases:

$$\begin{aligned}\Psi_{r\alpha} &= L_{\sigma r\alpha} i_{r\alpha} + \Psi_{\mu\alpha};\\ \Psi_{r\beta} &= L_{\sigma r\beta} i_{r\beta} + \Psi_{\mu\beta};\\ \Psi_{r\gamma} &= L_{\sigma r\gamma} i_{r\gamma} + \Psi_{\mu\gamma}.\end{aligned} \tag{7}$$

The electromagnetic torque of IM equation is

$$\begin{aligned}T_{\text{em}} = p\frac{\sqrt{3}}{2} M\big[&\left(i_{s\alpha} i_{r\gamma} + i_{s\beta} i_{r\alpha} + i_{s\gamma} i_{r\beta}\right)\\ &-\left(i_{s\alpha} i_{r\beta} + i_{s\beta} i_{r\gamma} + i_{s\gamma} i_{r\alpha}\right)\big].\end{aligned} \tag{8}$$

The equation of motion for the IM shaft in the case of single-mass mechanical part:

$$\frac{d\omega_r}{dt} = \frac{1}{J}(T_{em} - T_{load}), \tag{9}$$

where J is the moment of inertia of masses coupling with the rotor shaft and T_{load} is the static torque of mechanical load coupling with the IM shaft.

In the general case, Eq. (9) can be written as

$$\frac{d\omega_r}{dt} = \frac{1}{J}(T_{em} - T_{load}(t, \omega_r, \Theta_r)) = \frac{T_{dynamic}}{J}, \tag{10}$$

$T_{dynamic}$—dynamic torque on the IM shaft;

$$\omega_r = \omega_{r0} + \int_0^t \frac{T_{dynamic}}{J} dt, \tag{11}$$

ω_{r0}—initial angular speed of the rotor shaft of IM.

The angle of rotation of the IM rotor shaft, radian

$$\Theta_r = \Theta_{r0} + \int_0^t \omega_r dt, \tag{12}$$

Θ_{r0}—initial angular position of the IM rotor shaft, radian.

It is interesting to know the energy performance of the electric machine in the transition process. For IM in the absence of power from the rotor instantaneous value of the active power consumption is calculated as

$$P_1 = v_{s\alpha} i_{s\alpha} + v_{s\beta} i_{s\beta} + v_{s\gamma} i_{s\gamma}. \tag{13}$$

The instantaneous reactive power consumption

$$Q_1 = -\frac{1}{\sqrt{3}}\left[v_{s\alpha}\left(i_{s\beta} - i_{s\gamma}\right) + v_{s\beta}\left(i_{s\gamma} - i_{s\alpha}\right) + v_{s\gamma}\left(i_{s\alpha} - i_{s\beta}\right)\right]. \tag{14}$$

The instantaneous value of useful shaft power of IM

$$P_2 = \omega_r T_{\text{load}}. \tag{15}$$

The abovementioned equations (Eqs. (1)–(15)) of IM MM may be supplemented by the expressions (Eq. (16)), which allow to go to the description of the rotor

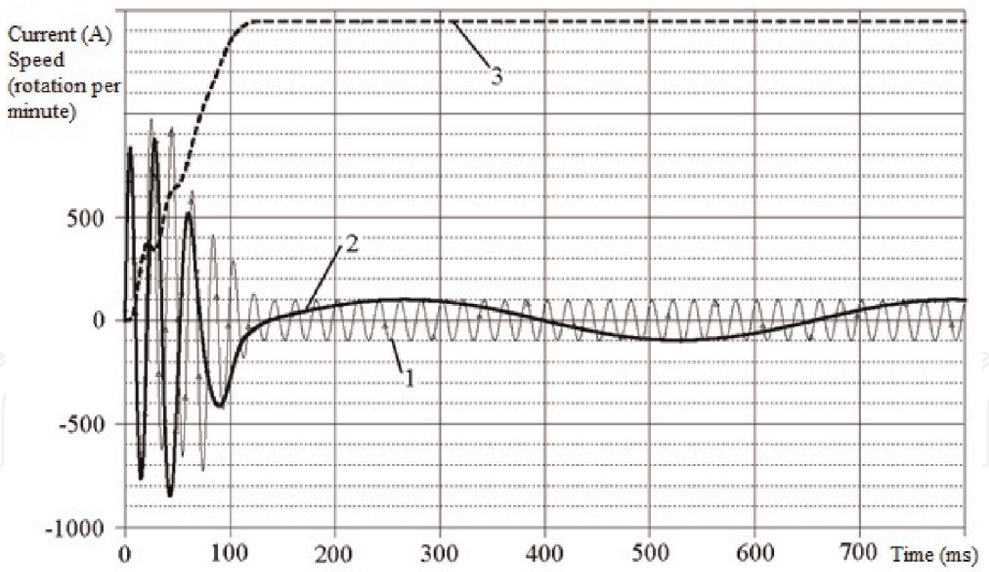


Figure 1.
The results of the rotor phase current simulation for IM type AE92-4.

phase currents at frequency of $f_2 = s \cdot f_1$, where s is the sleep of the rotor and f_1 is the frequency of stator voltage.

$$\begin{aligned}
i_{ra} &= i_{r\alpha}\left(\frac{1}{3}+\frac{2}{3}\cos\left(p\cdot\Theta_r\right)\right)+i_{r\beta}\left(\frac{1}{3}+\frac{2}{3}\cos\left(p\cdot\Theta_r-\frac{2\pi}{3}\right)\right)\\
&\quad+i_{r\gamma}\left(\frac{1}{3}+\frac{2}{3}\cos\left(p\cdot\Theta_r+\frac{2\pi}{3}\right)\right);\\
i_{rb} &= i_{r\alpha}\left(\frac{1}{3}+\frac{2}{3}\cos\left(p\cdot\Theta_r+\frac{2\pi}{3}\right)\right)+i_{r\beta}\left(\frac{1}{3}+\frac{2}{3}\cos\left(p\cdot\Theta_r\right)\right)\\
&\quad+i_{r\gamma}\left(\frac{1}{3}+\frac{2}{3}\cos\left(p\cdot\Theta_r-\frac{2\pi}{3}\right)\right);\\
i_{rc} &= i_{r\alpha}\left(\frac{1}{3}+\frac{2}{3}\cos\left(p\cdot\Theta_r-\frac{2\pi}{3}\right)\right)\\
&\quad+i_{r\beta}\left(\frac{1}{3}+\frac{2}{3}\cos\left(p\cdot\Theta_r+\frac{2\pi}{3}\right)\right)+i_{r\gamma}\left(\frac{1}{3}+\frac{2}{3}\cos\left(p\cdot\Theta_r\right)\right).
\end{aligned} \tag{16}$$

Such a representation of the rotor currents demonstrates the nature of changes in the transition processes (see **Figure 1**, which shows the results of the rotor phase current simulation in the case of balanced power supply sinusoidal voltages for IM type AE92-4, 4-pole, 40 kW). In **Figure 1**, curve 1 is $i_{r\gamma}$ current, curve 2 is i_{rc} current, and curve 3 is rotor speed. According to the frequency f_2, you can check the value of the rotor speed of IM.

Figure 2 shows the applicability of the developed MM for the simulation of electromagnetic and electromechanical processes in IM with its power supply from the power semiconductor converter—autonomous voltage inverter.

3. Requirements for computer model

In the process of the computer model of the IM according to the equations (Eqs. (1)–(12)), development using OrCAD—computer-aided design system—

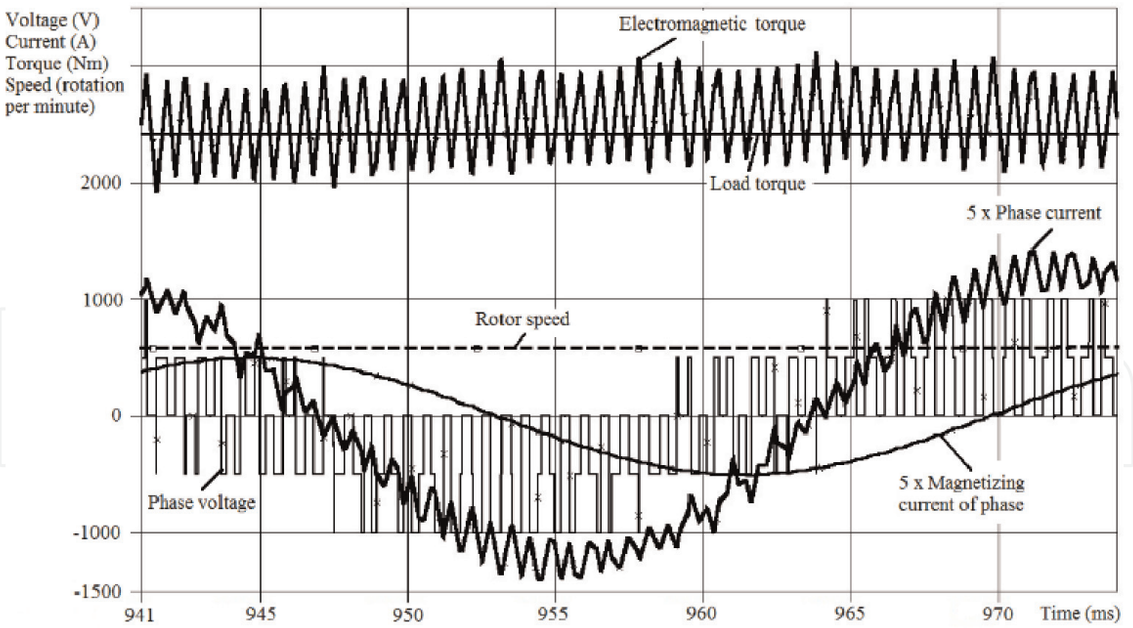


Figure 2.
The results of simulation for traction IM type DTA-350M (6-pole, 350 kW) under power supply from autonomous voltage inverter condition.

intended primarily for the design and simulation of electronic and electrical devices [8], there was the task of ensuring the embedded model of IM in an electrical power supply circuit, including converters, by simple connection of virtual terminals. That is, relative to the model of the electrical circuit that is attached to this circuit, the IM model should also have the properties of electric circuits: one can apply a potential difference to the terminals, providing a bidirectional electric current in the connecting circuits, including a pass-through current between them. Another task is the formation of such structure of the computer model which will be used perhaps as a universal template, which records the values of variables (parameters of IM), asked simultaneously for all equations. The resulting computer model is suitable for the description of both the squirrel-cage and wound rotor IM in any of four quadrants. The winding phases can be connected in a triangle scheme, wye, independently joined with each of its voltage to have any other wiring of each other or of power source. The developed computer model gives the user access to the beginning and the end of a winding of each of the three phases of the stator and the rotor. This property is particularly important when considering the asymmetric modes of operation or when powered by the special circuitry of semiconductor converters [9].

4. The implementation of a computer model

The tasks are solved by combining two approaches in the IM computer model development: circuit for electrical parts and the method of block diagrams for the magnetic and mechanical parts. The computer model of IM is packed into a hierarchical block with a specified list of variables (parameters of IM). Within a single OrCAD project, using the copy operation, one can get the required number of hierarchical blocks (models of IM), for each of which it is possible to set unique parameter values. Sensors and signal inputs in the IM model used controlled sources of currents and voltages. Such voltage source is controlled by current (VSCC) and by voltage (VSCV), and current source is controlled by voltage (CSCV). A graphical image of the computer model of phase *A* windings of the stator and the rotor of IM, composed of Eqs. (1)–(7), is shown in **Figure 3**.

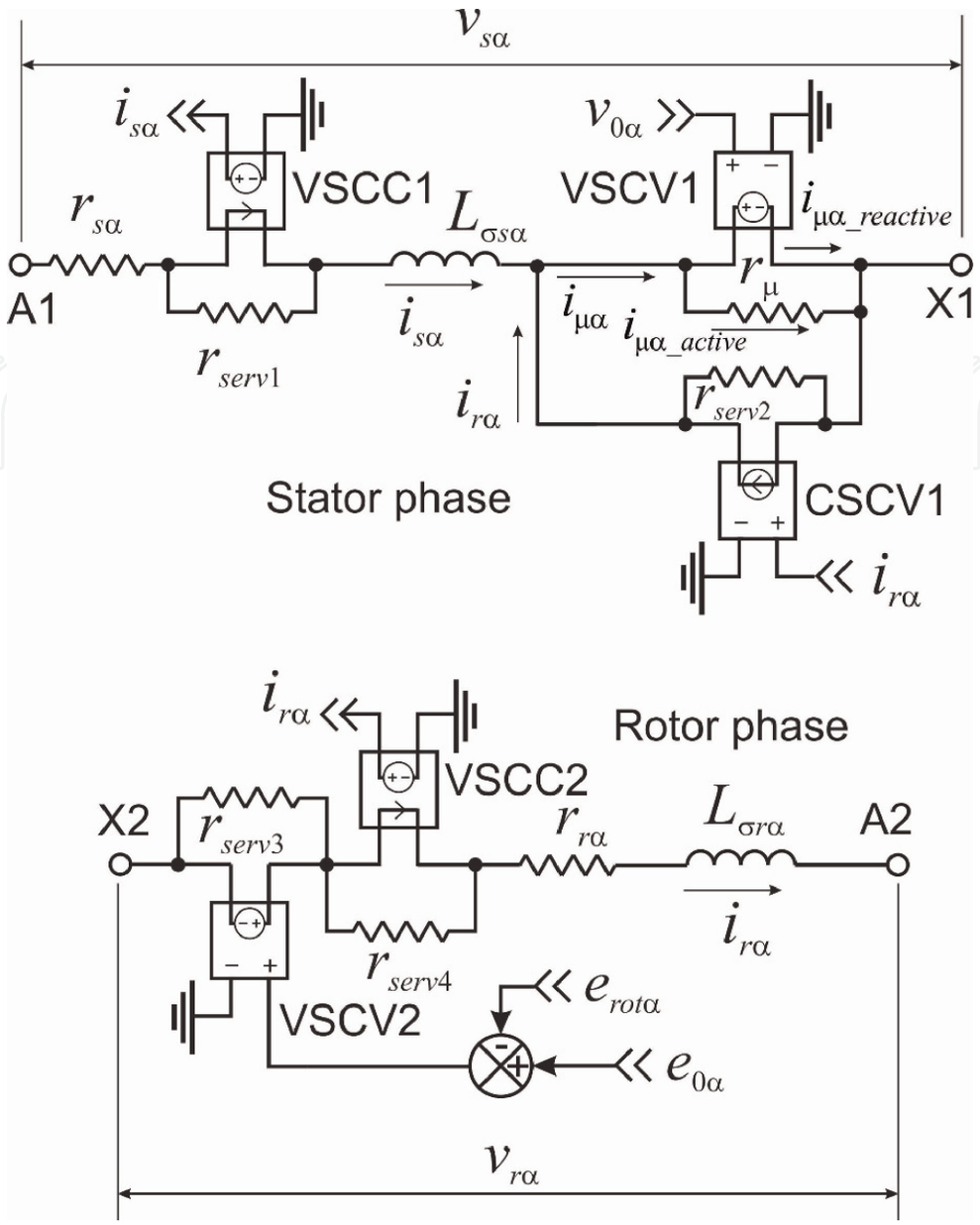


Figure 3.
The graphical image of the computer model of phase A *windings of the stator and the rotor of IM.*

VSCC1 performs a function of the phase current of the stator $i_{s\alpha}$ sensor; similarly, VSCC2 is a sensor of rotor phase current $i_{r\alpha}$ given to the stator winding. CSCV1 is used for entering $i_{r\alpha}$ into the scheme. VSCV1 is introduced into the phase magnetizing circuit $v_{0\alpha}$ voltage. A similar function is performed by VSCV2 entering into the circuit of the rotor winding; the difference is between the electromotive force of a branch of magnetization and rotation electromotive force, i.e., the voltage drop value. Active resistances r_{serv} (see **Figure 3**) have a large value, for example, 10 MΩ. These resistors are introduced for service purposes. Without affecting numerical calculation results, they stabilize the solution (simulation) by maintaining the current circuit (the physical sense—the way for leakage current), which is especially important when a discrete change of the resistance of a IM circuit occurs, for example, when powered from the frequency converter or in the case of the phase circuit breaking. A similar solution is described in [10].

The rest of the equations of a three-phase IM mathematical model is implemented by the author in the computer model in the form of block diagrams [11]. **Figure 4** shows a part of the model, where one obtains instantaneous value of $L_{\mu}*$—complete phase inductance of the stator winding from the main magnetic

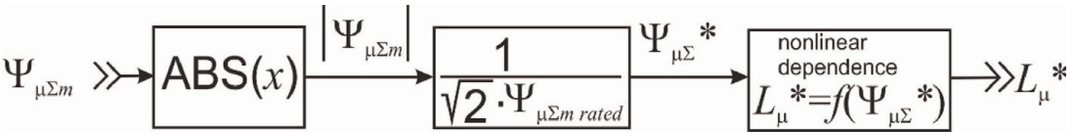


Figure 4.
The block diagram for obtaining instantaneous values of complete phase inductance of the stator winding from the main magnetic flux in relative units $L_\mu*$.

flux in relative units. $\Psi_{\mu\Sigma mrated}$ is the rated value of $\Psi_{\mu\Sigma m}$—the instantaneous value of the amplitude of the representing vector of the flux linkage of mutual induction.

Signal $\Psi_{\mu\Sigma m}$ can be calculated as

$$\Psi_{\mu\Sigma m} = \sqrt{\Psi_{\mu x}^2 + \Psi_{\mu y}^2}, \tag{17}$$

where $\Psi_{\mu x}$ and $\Psi_{\mu y}$ are the projections of the representing vector of the flux linkage of mutual induction on orthogonal coordinate axes X and Y. In the case of three-phase stator reference frame of the coordinate system axis, these projections are derived from mutual induction flux linkages of each phase.

$$\Psi_{\mu x} = \frac{2}{3}\left(\Psi_{\mu\alpha} + \Psi_{\mu\beta}\cos\left(-\frac{2\pi}{3}\right) + \Psi_{\mu\gamma}\cos\left(\frac{2\pi}{3}\right)\right); \tag{18}$$

$$\Psi_{\mu y} = -\frac{2}{3}\left(\Psi_{\mu\beta}\sin\left(-\frac{2\pi}{3}\right) + \Psi_{\mu\gamma}\sin\left(\frac{2\pi}{3}\right)\right). \tag{19}$$

Figure 5 shows the piecewise linear approximation by five points of $L_\mu*\left(\Psi_{\mu\Sigma}*\right)$ for IM type AGV250 (2-pole, 110 kW). Such a way successfully tested in IM simulator is developed by means of OrCAD PSpice [8]: the one standard component table is used for programming the abovementioned approximated dependence.

In **Figure 6** there is the model part corresponding to the abovementioned (Eqs. (1)–(3)) equations. **Figure 7** shows a part of the IM model, designed to determine the rotation electromotive force in each phase. Model rotor speed ω_{r_model} in p times is higher than the real mechanical speed of rotor ω_r. **Figure 8** shows a

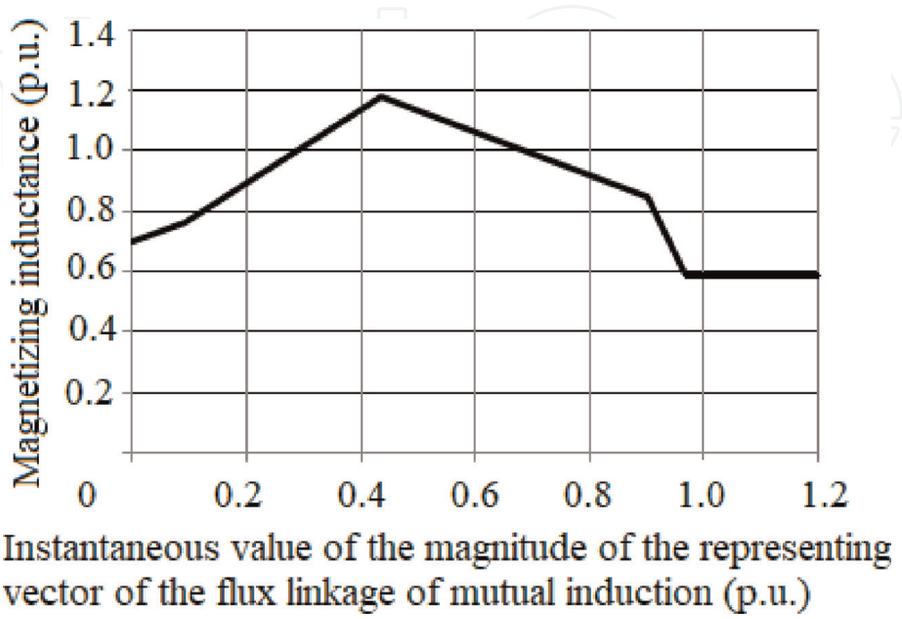


Figure 5.
The piecewise linear approximation by five points of $L_\mu*\left(\Psi_{\mu\Sigma m}*\right)$ for IM type AGV250.

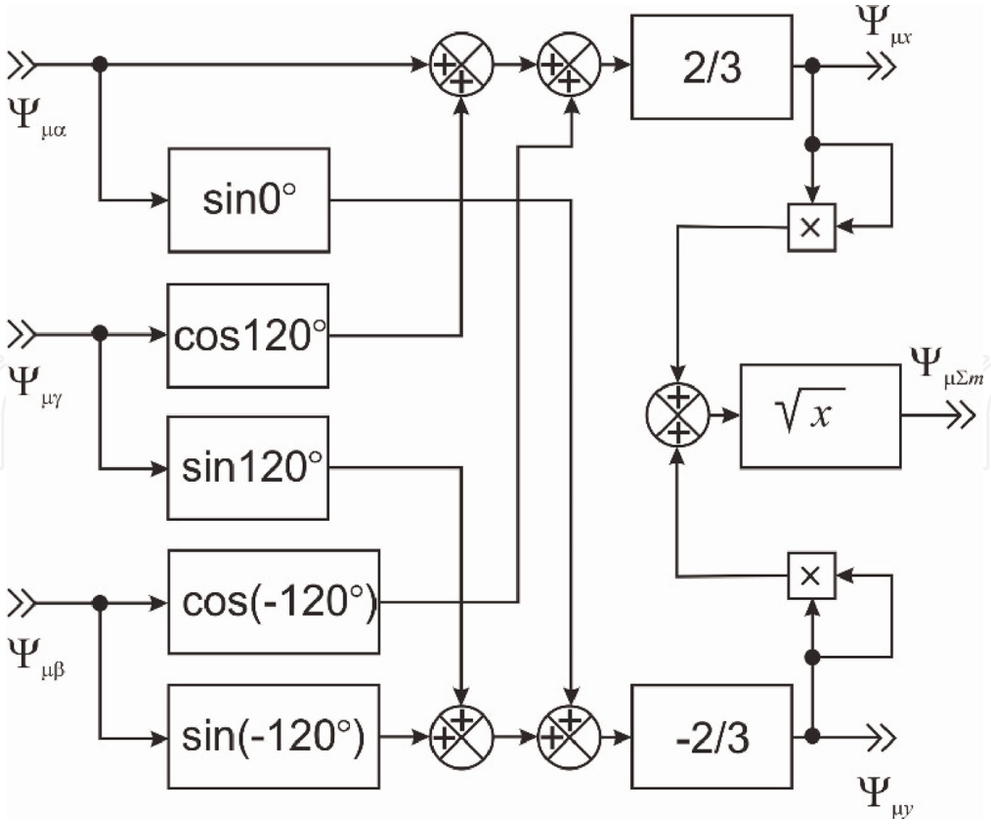


Figure 6.
The block diagram that implements the calculation of the instantaneous value of the amplitude of the representing vector of the flux linkage of mutual induction.

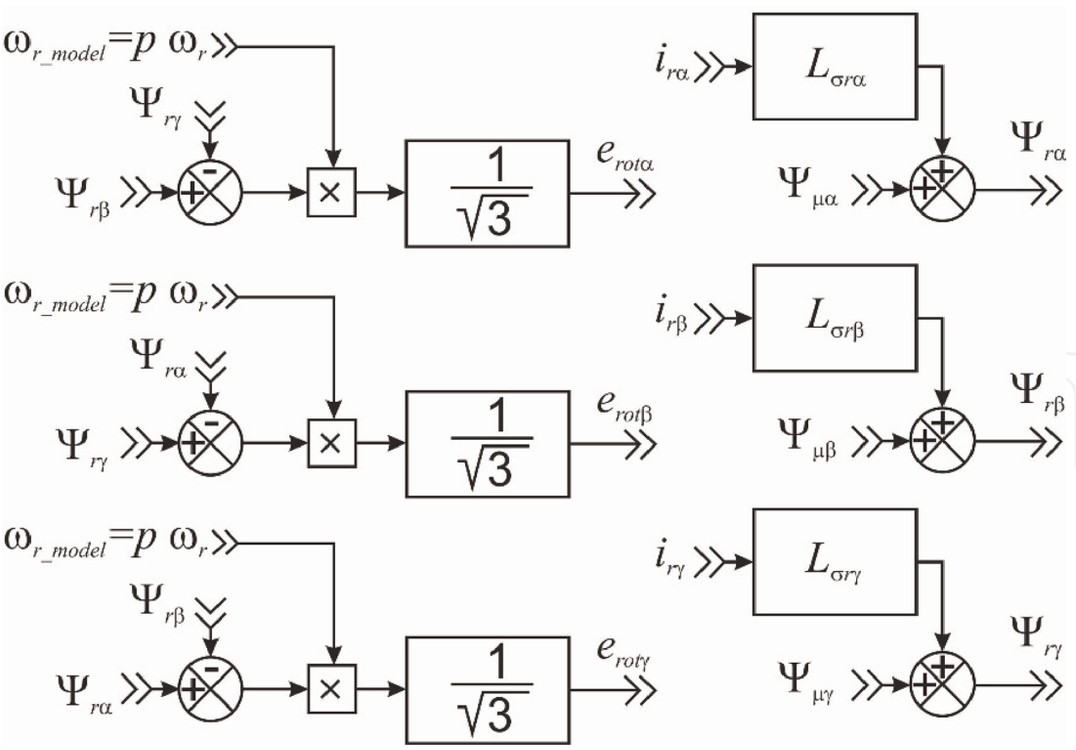


Figure 7.
Part of the IM model, designed to determine the rotation electromotive force in each phase.

part of the IM model corresponding to equations (Eq. (2)). **Figure 9** shows a part of the model, which forms the signals of electromagnetic torque T_{em}, angular speed ω_r, and the angle of rotation Θ_r of the rotor. In **Figure 9**, n_r is mechanical angular rotor speed, rotation per minute.

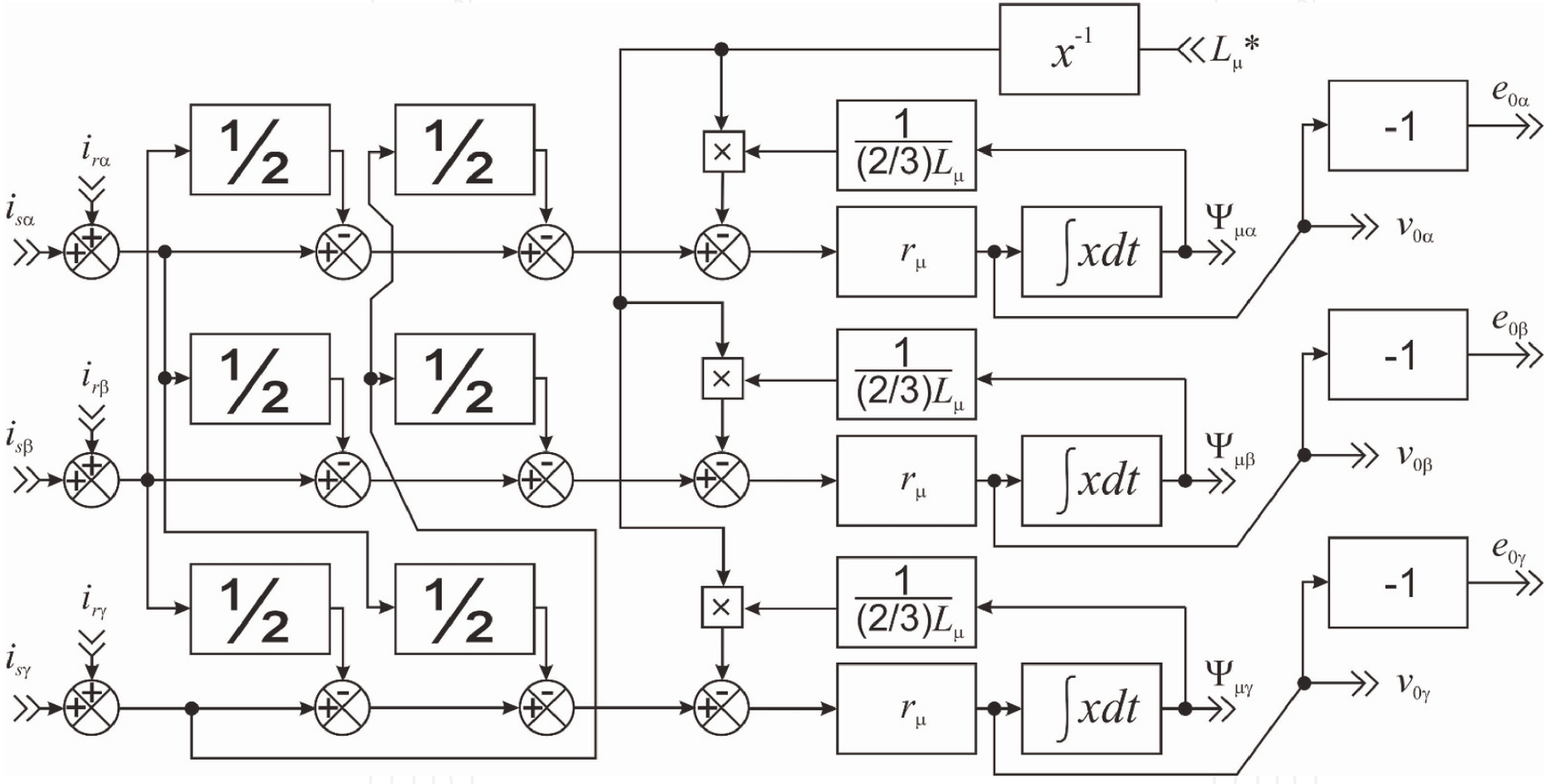


Figure 8.

Block diagrams corresponding to equations (Eq. (2)).

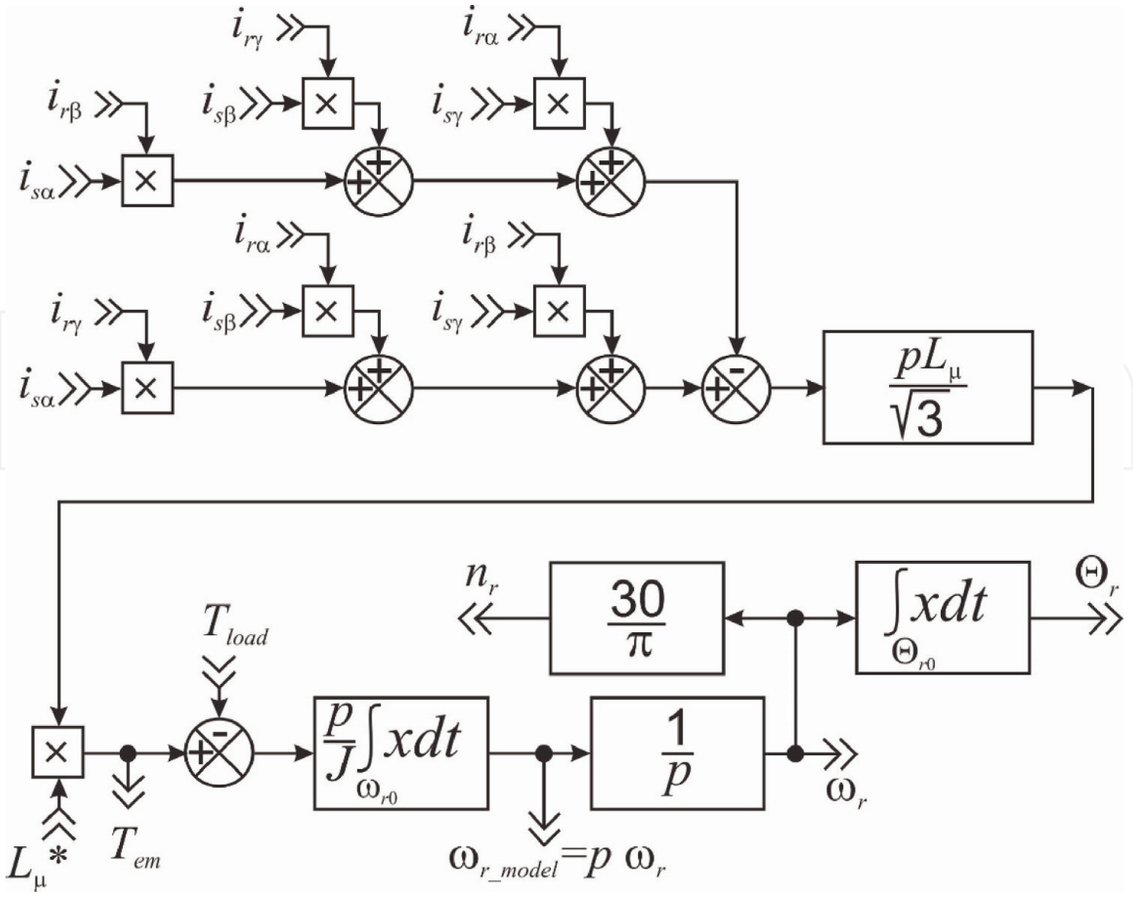


Figure 9.
Block diagrams, which form the signals of electromagnetic torque T_{em}, angular speed ω_r, and the angle of rotation of rotor Θ_r.

5. An example of using a mathematical model of the motor when the power supply voltage is unbalanced

A good example of functionality for previously provided MM under unbalanced supply voltage maybe modeling of electromechanical phase splitter, made on the basis of a three-phase IM.

Electromechanical phase splitters are used in Russia and India [12] onboard of electric trains and electric locomotives for transform AC single-phase voltage in three-phase voltage to feed auxiliary electric drives with IM loaded by fans and air compressors. **Figure 10** is a schematic diagram of the rotary phase splitter, where C_1 is operating and C_2 is start-up capacity.

Phase splitters are IM with a symmetrical or nonsymmetrical stator winding and no load (or low load) on the shaft. Phase splitter can be considered as combined single-phase IM and three-phase synchronous generator. In accordance with the terminology, adopted in India, the phase splitter is called the ARNO converter [12].

On contemporary freight AC electric locomotives of family "Ermak" in Russia, IM of NVA-55 type (4-pole, 55 kW) is used as a phase splitter. To drive the fans and compressor, the same type of IM is used. Let us make simulation of the phase splitter start without connecting electrical loads to check for phase splitting effect. Define $C_1 = 968$uF and $C_2 = 2904$uF. The torque of mechanical losses on the shaft (of the load) will take 28 Nm at the rotor speed of 1500 rotation per minute.

The simulated results of phase splitter start are shown in **Figures 11** and **12**, where the graphs are 1, 2, 3—line voltages between phases *A-B*, *B-C*, *C-A*— and 4, rotor speed. Start-up capacity C_2 is switched off when the current value of the

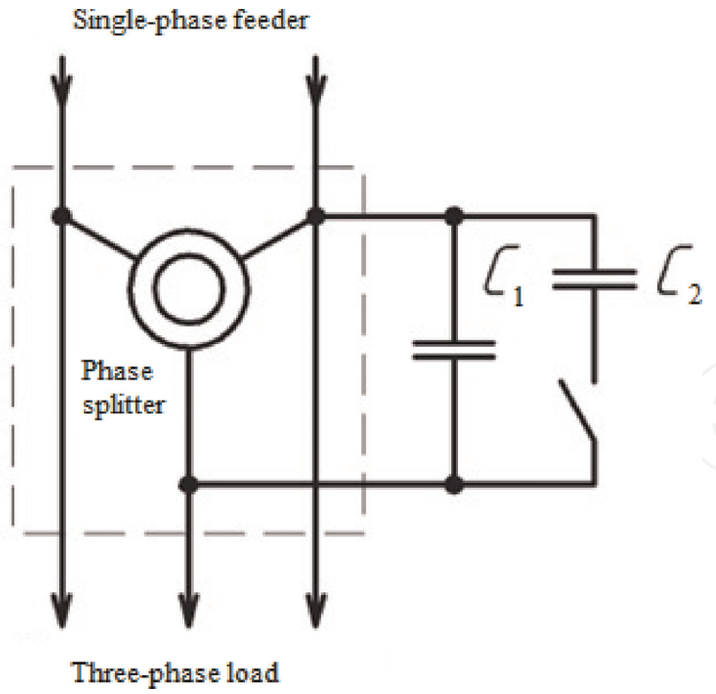


Figure 10.
Schematic diagram of the rotary phase splitter.

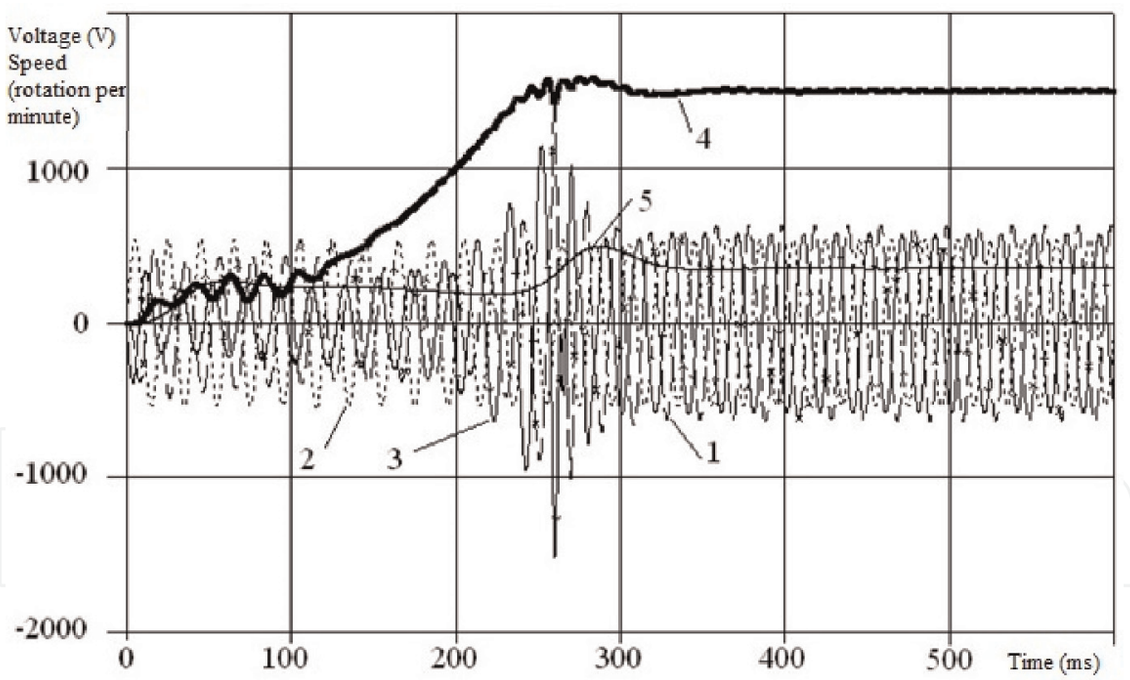


Figure 11.
Results of phase splitter start simulation.

voltage between one of the wires of a single-phase supply and wire of the phase splitter stator winding phase, which is not connected to single-phase supply (see **Figure 10**), will be over the value of 300 volts—such a situation means the end of the rotor acceleration and ending the formation of a three-phase voltage system (signal 5 in **Figure 11**).

Figure 12 shows the results of simulation of phase splitting in steady state (at average rotor speed of phase splitter 1500 rotation per minute). In **Figure 12** curves 6–8 are the phase currents A, B, and C. **Table 1** presents the numerical results at

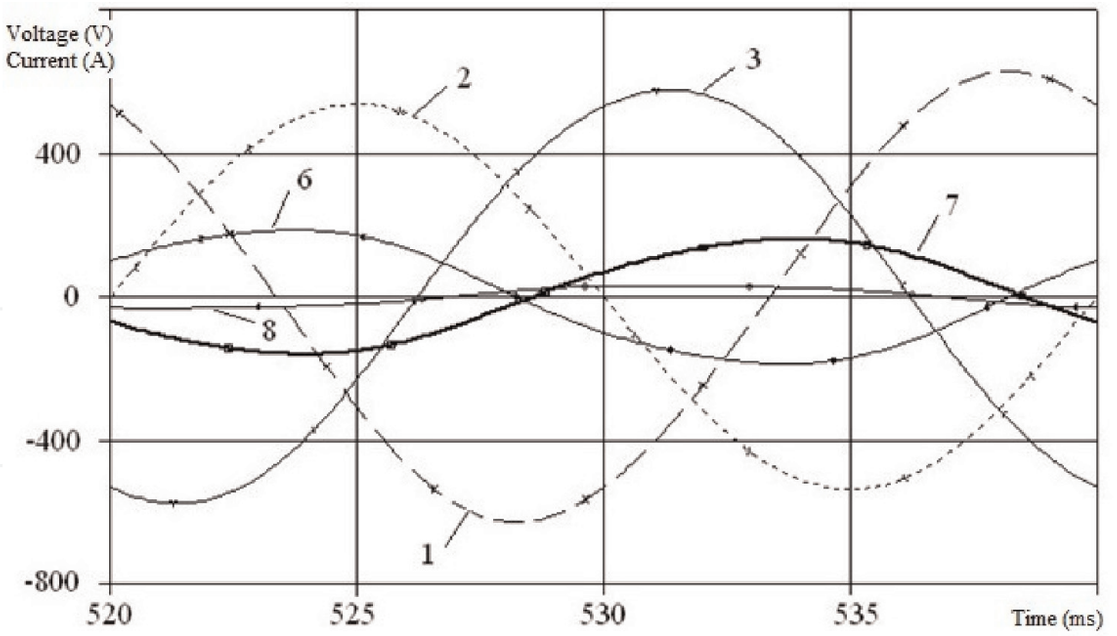


Figure 12.
Results of phase splitter simulation at steady-state mode.

Phase-to-phase voltages (V)			Phase currents (A)		
A-B	*B-C*	*C-A*	*A*	*B*	*C*
444	380	408	131.9	113.9	22.1
Splitted	Obtained from a single-phase transformer secondary winding	Splitted	Without any connected electrical loads		

Table 1.
Results of phase splitter simulation at steady-state mode.

steady-state mode. Obviously, the phase splitting effect is clearly demonstrated by the results of simulation.

The proposed mathematical model of a three-phase IM and the method of its computer implementation confirmed their adequacy and effectiveness to address some of the problems of analysis and design of electrotechnical complexes and systems, having IM in its composition.

6. Conclusion

In conclusion, the author would like to identify ways of improving the suggested mathematical model of a three-phase IM [13, 14]. Priority for criticism might be the lack in the mathematical model accounting for the skin effect in the conductors of the rotor winding. In fact, this is a notable disadvantage since in some cases, the current displacement in the rotor is able to accelerate the transitional process of IM start-up in several times [15, 16].

There are two types of problems whose solution requires a mathematical model accounting for the skin effect in the conductors of the IM rotor winding: the correct description of transient processes at direct start-up and correct account of the losses in the rotor winding in the case of feeding from the source of non-sinusoidal voltage or current. When deciding tasks of the first type, the author sometimes puts active resistance and leakage inductive resistance of the rotor, which change depending on

the slip. The solution of tasks of the second type requires the coordination of the complex resistance components of the rotor values to current frequency in it. The second approach is more versatile as it can be used for solution of both types of the abovementioned tasks. According to the author, to implement the second approach, the best way is to create the computer implementation of the mathematical model of a three-phase IM in the original coordinates.

IntechOpen

IntechOpen

Author details

Mikhail Pustovetov
Don State Technical University, Rostov-on-Don, Russian Federation

*Address all correspondence to: mgsn2006@rambler.ru

IntechOpen

© 2019 The Author(s). Licensee IntechOpen. This chapter is distributed under the terms of the Creative Commons Attribution License (http://creativecommons.org/licenses/by/3.0), which permits unrestricted use, distribution, and reproduction in any medium, provided the original work is properly cited. CC BY

References

[1] Ikeda M, Hiyama T. Simulation studies of the transients of squirrel-cage induction motors. IEEE Transactions on Energy Conversion. 2007;**22**(2):233-239

[2] Diaz A, Saltares R, Rodriguez C, Nunez R, Ortiz-Rivera E, Gonzalez-Llorente J. Induction motor equivalent circuit for dynamic simulation. In: Proceedings of the Electric Machines and Drives Conference (IEMDC '09); New York: IEEE International; 2009. pp. 858-863

[3] Sreedevi M, Jeno Paul P. Stator fault detection and diagnosis of an induction motor using neuro fuzzy logic. International Journal of Electrical and Power Engineering. 2011;**5**(2):102-107

[4] Hung R, Dommel H. Synchronous machine models for simulation of induction motors transients. IEEE Transactions on Power Systems. 1996; **11**(2):833-838

[5] Kopylov I. Mathematical Modeling of Electrical Machines. 2nd ed. Moscow: Vyshaya Shkola; 1994. 318 p

[6] Sokola M, Levi E. A novel induction machine model and its application in the development of an advanced vector control scheme. International Journal of Electrical Engineering Education. 2000; **37**(3):233-248

[7] Pustovetov M. A universal mathematical model of a three-phase transformer with a single magnetic core. Russian Electrical Engineering. 2015; **86**(2):98-101

[8] Keown J. OrCAD PSpice and Circuit Analysis. 4th ed. Upper Saddle River, New Jersey, Columbus, Ohio: Prentice Hall; 2001. 609 p

[9] Halina T, Stalnaya M, Eremochkin S, Ivanov I. Modeling electromechanical characteristics of three-phase motors with inverters vector: Algorithmic type in Matlab Simulink environment. Procedia Engineering. 2016;**165**: 995-1005

[10] Zirka S, Yu M, Arturi C. Accounting for the influence of the tank walls in the zero-sequence topological model of a three-phase, three-limb transformer. IEEE Transactions on Power Delivery. 2014;**29**(5):2172-2179

[11] Ogata K. Modern Control Engineering. 5th ed. Prentice Hall; 2010. 894 p

[12] Arunodai C. Use of Arno converter and motor generator set to convert a single-phase AC supply to a three-phase AC for controlling the speed of a three-phase induction motor by using a three-phase to three-phase cycloconverter. International Journal of Electrical Engineering & Technology. 2016;7(2): 19-28

[13] Pustovetov M. A mathematical model of the three-phase induction motor in three-phase stator reference frame describing electromagnetic and electromechanical processes. In: Proceedings of the IEEE Conference Dynamics of Systems, Mechanisms and Machines (Dynamics '16); 15-17 November 2016; Omsk. New York: IEEE; 2016. DOI: 0.1109/ Dynamics.2016.7819069

[14] Pustovetov M. Approach to computer implementation of mathematical model of 3-phase induction motor. In: IOP Conference Series: Materials Science and Engineering 327; 2018. 022085. DOI: 10.1088/1757-899X/327/2/022085

[15] Maksimkina J. Direct start-up of the squirrel-cage induction motor at

variable parameters of the rotor. Latvian Journal of Physics and Technical Sciences. 2013;**50**(1):10-21

[16] Benecke M, Doebbelin R, Griepentrog G, Lindemann A. Skin effect in squirrel cage rotor bars and its consideration in simulation of non-steady-state operation of induction machines. PIERS Online. 2011;**7**(5): 421-425

IntechOpen

IntechOpen